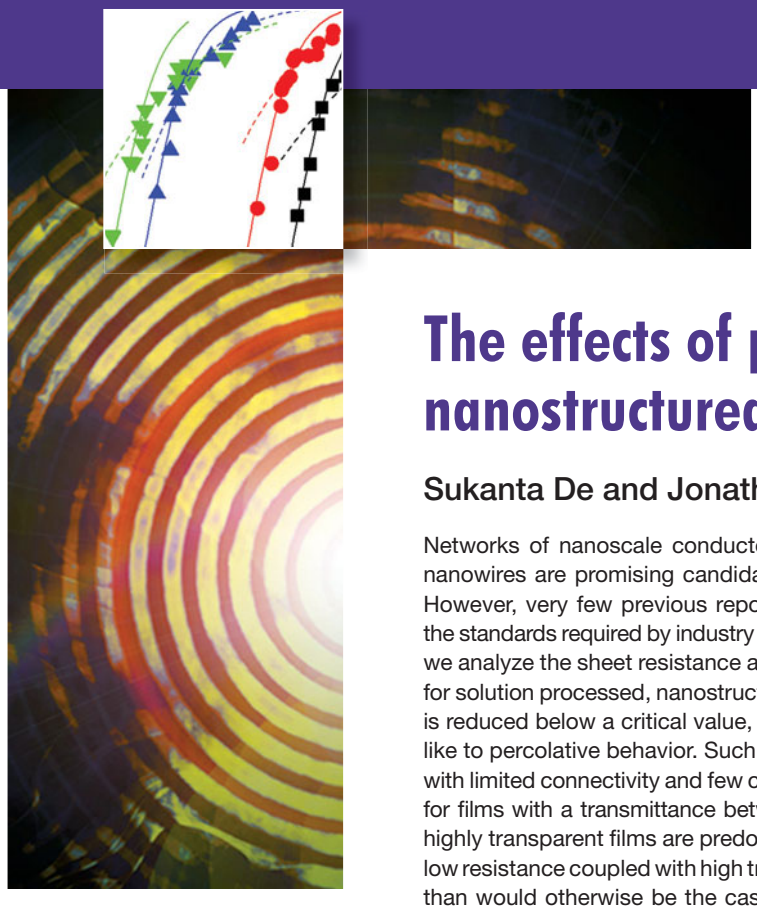

The effects of percolation in nanostructured transparent conductors

Sukanta De and Jonathan N. Coleman

Networks of nanoscale conductors such as carbon nanotubes, graphene, and metallic nanowires are promising candidates to replace metal oxides as transparent conductors. However, very few previous reports have described nanostructured thin films that reach the standards required by industry for high-performance transparent electrodes. In this review, we analyze the sheet resistance and transmittance data extracted from published literature for solution processed, nanostructured networks. In the majority of cases, as their thickness is reduced below a critical value, nanoconductor networks undergo a transition from bulk-like to percolative behavior. Such percolative behavior is characteristic of sparse networks with limited connectivity and few continuous conductive paths. This transition tends to occur for films with a transmittance between 50% and 90%, which means that the properties of highly transparent films are predominately limited by percolation. Consequently, to achieve low resistance coupled with high transparency, the networks must be much more conductive than would otherwise be the case. We show that highly conductive networks of metallic nanowires appear to be the most promising candidate to replace traditional transparent electrode materials from a technical standpoint. However, many other factors, including cost, manufacturability, and stability, will have to be addressed before commercialization of these materials.

Introduction

In the modern world, transparent conductors (TCs) are extremely common. They are generally found as thin films that have low electrical resistance but are optically transparent and are critically important in many modern electronic devices. In the home or office, they are found in flat panel displays such as in TVs, laptops or digital cameras, as smart windows, heat shields in some oven windows, and as invisible security circuitry on glass windows. They defrost windows in planes, trains, and automobiles and are used in self-dimming rearview mirrors in cars. They are also used in portable electronic devices (phones, tablet computers) that affect our daily lives. Many people hope that as electrodes in solar cells, they will help generate clean, renewable energy.

Modern TC technology is dominated by doped metal oxides, of which the most important is tin-doped indium oxide (ITO).[1–3] This material has been studied for 80 years[3] and has been largely optimized for a range of properties. For example, while metal oxide TCs can display transmittances as high as 95% and sheet resistances as low as 3 Ω/sq, they also have a range of other useful properties, such as work functions that vary between 4.2 and 5.3 eV, depending on the material, thermal stability, and chemical and mechanical durability.[2] In fact, metal oxides are model materials for transparent electrodes. However, even model systems may fall victim to issues related to limited supply and ever growing demand.

Partly due to the rapid growth in portable electronics, the demand for ITO is currently growing at 20% per annum. Due to a combination of this demand and the already limited supply, the cost of indium and hence ITO has risen dramatically in recent years (see Reference 3 and references therein). Furthermore, metal oxides have another weakness: brittleness.[4–7] It is thought that a significant fraction of future displays will be plastic-based and inherently flexible. As metal oxides tend to fracture at strains of ~2%, they are completely unsuitable for use in such flexible electronics. Other problems with metal oxides include their high refractive index and the high cost of producing large area metal oxide coated glass.

Thus, it is clear that new transparent conducting materials are required. These must have a number of specific properties:

Sukanta De, Center for Research in Adaptive Nanostructures and Nanodevices, and School of Physics, Trinity College Dublin, Ireland; desu@tcd.ie
Jonathan N. Coleman, Center for Research in Adaptive Nanostructures and Nanodevices and School of Physics, Trinity College Dublin, Ireland; colemaj@tcd.ie
DOI: 10.1557/mrs.2011.236

they must retain their electrical conductivity after repeated flexing; it must be possible to deposit them over large areas using low-temperature processing; they must have deposition and material costs comparable to ITO; and, most importantly, they must match ITO in terms of optoelectrical properties. For example, it must be possible to form these materials into films with $T > 90\%$. This is not challenging, as any material can be made extremely transparent just by making it sufficiently thin. The most difficult goal is finding a material that has high enough electrical conductivity such that, even when formed in a very thin film, it displays sheet resistance low enough to be useful.

How low is low enough? ITO fulfills a wide range of roles, all of which require high transparency. However, each role has a particular resistance requirement, with the entire set spanning a wide range. For example, conducting films for static dissipation can function with a sheet resistance of >1 kΩ/sq;[2] touch screens generally require a few hundred Ω/sq;[3] electrodes require a few tens of Ω/sq;[8] while, to minimize resistive losses, solar cell electrodes require sheet resistances of <10 Ω/sq.[9] We make the assumption that it will not be difficult to find materials that fulfill the less stringent, high sheet resistance applications. For example, a range of nanostructured materials have achieved transmittance above 90% coupled with sheet resistance above 1 kΩ/sq. However, achieving transmittance above 90% coupled with sheet resistance below 200 Ω/sq has proven much more difficult. Thus, in this article, we focus on the search for high-performance, solution-processed TCs that are usually, and somewhat arbitrarily, defined as those with a transmittance of $T \geq 90\%$ and a sheet resistance of $R_s \leq 100$ Ω/sq.[10]

In the race to develop materials that fulfill these criteria, many researchers have focused on networks of conducting nanomaterials such as carbon nanotubes (CNTs),[11–35] metal nanowires,[36–42] and disordered arrays of exfoliated graphene flakes.[43–63] Such networks are particularly useful, as they can be deposited at low temperatures from solution using industry-friendly techniques such as spraying.[14,39,44,64,65] Taking nanotube networks as an example, because adjacent tubes interact only weakly, intertube junctions can move locally under strain. As intertube charge transport is independent of junction position, the electrical properties tend to be independent of strain, resulting in great electrical stability under flexing.[13,35,36,46] In addition, extremely sparse networks can be produced, resulting in very high transmittances.[65] Indeed, such nanostructured networks look ideal as future ITO replacement materials. However, there is one outstanding problem; very few previous studies have demonstrated nanostructured networks that are thin enough to display $T \geq 90\%$ and $R_s \leq 100$ Ω/sq.[37,39,41]

Thus, it is critical to assess the progress in the field. In this work, we will compare the published performance of transparent conductors produced from networks of single-walled carbon nanotubes (SWNTs),[11–35] graphene flakes,[43–63] and metallic nanowires[10,36–42] (see supporting information for detailed tabulated data). Keeping in mind the requirement for low-temperature, large-area deposition, we will focus on solution-processed networks. We will demonstrate which materials are most promising and show that to demonstrate high performance, it is important to have both the correct materials and the correct network properties.

Bulk versus percolative behavior

Researchers have been studying nanostructured materials for transparent electrodes for over six years.[15,16,66] The technology is now mature enough to compare and contrast the various materials under study. It is often helpful to use figures of merit (FoM) to express the performance of a given film type and facilitate comparison with other data sets. The most useful FoMs are those that are based on the physics of the system under study. For example, FoMs for TCs should link the film transmittance, T, to its sheet resistance, R_s. This is done by combining physical expressions for transmittance and sheet resistance of thin films, both as a function of thickness, t. For example, the transmittance can be expressed as[67]

$$T = \left(1 + \frac{Z_0}{2}\sigma_{op}t\right)^{-2}, \quad (1)$$

where Z_0 is the impedance of free space (377 Ω), and σ_{op} is the optical conductivity (related to the absorption coefficient α as $\sigma_{op} \approx \alpha/Z_0$).[12] By combining this expression with the definition of sheet resistance (for a bulk-like film):

$$R_s = \left(\sigma_{dc,B}t\right)^{-1} \quad (2)$$

($\sigma_{dc,B}$ is the bulk dc conductivity of the film) to eliminate t, one obtains a relationship between T and R_s:

$$T = \left[1 + \frac{Z_0}{2R_s}\frac{\sigma_{op}}{\sigma_{dc,B}}\right]^{-2}. \quad (3)$$

Note that this expression is appropriate for a bulk-like material (i.e., one whose dc conductivity is invariant with sample thickness). The conductivity ratio $\sigma_{dc,B}/\sigma_{op}$ is often used as a FOM for transparent conductors as high values of $\sigma_{dc,B}/\sigma_{op}$ lead to films with high T and low R_s. In fact, a material with a given value of $\sigma_{dc,B}/\sigma_{op}$ can be formed into films with a range of T and R_s values depending on the thickness. Thus in practice, researchers generally prepare films with a range of thicknesses, measure R_s and T for each thickness, and then fit the (T, R_s) data to Equation 3 to extract $\sigma_{dc,B}/\sigma_{op}$. Examples of this procedure are shown in **Figure 1**. Here, transmittance is plotted as a function of sheet resistance for thin films of graphene,[55] SWNTs,[34] Cu nanowires,[41] and Ag nanowires.[36] In each case, the bottom left portion of the data (corresponding to thicker films) is fit to Equation 1 (solid lines), giving values of $\sigma_{dc,B}/\sigma_{op}$ of 0.25, 1.5, 110, and 415, respectively. Usually these numbers are assumed to encode all the relevant information about the optoelectrical properties of these films. In order to achieve the target of $T \geq 90\%$ and $R_s \leq 100$ Ω/sq, Equation 3 can be used to show that $\sigma_{dc,B}/\sigma_{op} \geq 35$ is required.

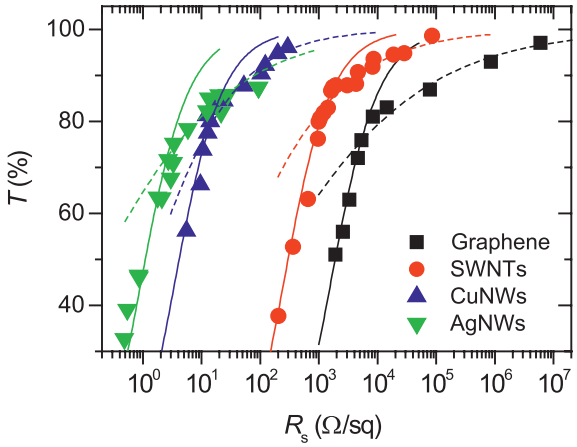

Figure 1. Typical graph of transmittance (generally measured at ~550 nm) plotted versus sheet resistance for thin films of nanostructured materials. Note that each curve can be divided into two regimes, the bulk regime (the solid line is a fit to Equation 3) and the percolation regime (the dashed line is a fit to Equation 5).[34,41,55,63]

This is the first criterion for a high-performance transparent conductor.

However, looking carefully at the fits in Figure 1, it is clear that the data tend to deviate severely from the fits for thinner (more transparent) films. This deviation has been observed before[13,14,35,36,46,68] and tends to occur for films with T between 50% and 92% (see later in text). This is important because applications requiring TCs usually require $T \geq 90\%$. Thus, $\sigma_{dc,B}/\sigma_{op}$ fails to describe the relationship between T and R_s in the technologically relevant regime. This means that in many cases, $\sigma_{dc,B}/\sigma_{op}$, or indeed any FoMs based on bulk properties, are not entirely appropriate, particularly when high transparency is required. Recently, it has been shown that the deviation from bulk-like behavior as described in Equation 1, can be explained by percolation effects.[68] Such effects become important for very sparse networks of nanoconductors. When the number of nanoconductors per unit is very low, a continuous conducting path from one side of the sample to the other will generally not exist. As more nanoconductors are added, at some point (the percolation threshold) the first conducting path will be formed. As more material is added, more conductive paths are formed, and the conductivity of the network increases rapidly. Eventually it reached a "bulk-like" value above which it remains constant. Percolation theory describes how the dc conductivity of sparse networks depends on network thickness and predicts a non-linear, power law dependence:[69]

$$\sigma_{dc} \propto (t - t_c)^n, \quad (4)$$

where t is the estimated thickness of the network, t_c is the thickness associated with the percolation threshold, and n is the percolation exponent. This leads to a new relationship between T and R_s, which applies to thin, transparent networks:[68]

$$T = \left[1 + \frac{1}{\Pi}\left(\frac{Z_0}{R_s}\right)^{1/(n+1)}\right]^{-2} \quad (5)$$

where Π is the percolative FoM:

$$\Pi = 2\left[\frac{\sigma_{dc,B}/\sigma_{op}}{(Z_0 t_{min}\sigma_{op})^n}\right]^{1/(n+1)}. \quad (6)$$

Here, t_{min} is the thickness below which the dc conductivity becomes thickness dependent (i.e., Equation 5 applies below t_{min} but Equation 3 applies above t_{min}). Analysis of these equations shows that large values of Π but low values of n are desirable to achieve low R_s coupled with high T.[68] Furthermore, networks of nanostructures show values of t_{min}, which scale closely with the nanostructures' smallest dimension, D: $t_{min} \approx 2.33D$.[68] The high T portion of data in Figure 1 were fitted using Equation 5. In all cases, good fits allow the calculation of both n and Π. It is clear from this analysis that knowledge of n and Π is critical to understanding the behavior of thin networks of nanostructured materials (i.e., those in the technologically relevant regime). However, while n is a fundamental property of the network, looking at Equation 6, we note that Π is a composite parameter that is related to $\sigma_{dc,B}/\sigma_{op}$. This means that while $\sigma_{dc,B}/\sigma_{op}$ does not directly control T and R_s in the high T regime, it is certainly of indirect importance. In this article, we describe both $\sigma_{dc,B}/\sigma_{op}$ and the percolation parameters, n and Π, for a range of previously reported nanostructured TCs.

Analysis of literature data

The aim of this article is to assess the relative merits and to understand the limitations of the nanomaterials commonly used to prepare TCs. To this end, we extracted data for (R_s, T) from a range of studies describing transparent conducting properties of thin films of graphene, SWNTs, and metallic nanowires (tabulated data are included in the supporting information). The graphene data included films of solution-cast reduced graphene oxide and surfactant exfoliated graphene but no vapor grown graphene. In the majority of cases, the data contained both bulk and percolation regimes. Each regime was fitted to the relevant equation (3 or 5) and values for $\sigma_{dc,B}/\sigma_{op}$, n and Π were extracted. We note that we have not analyzed every paper in the literature; however, we hope that the range of papers studied and cited herein roughly captures the current state of the field.

We begin by looking at the extracted values of $\sigma_{dc,B}/\sigma_{op}$. For each material, the conductivity ratio was ranked from highest (i.e., number 1) to lowest (i.e., number 45 for nanotubes). The position in this ranking list is known as the ratio ranking. The conductivity ratio values are plotted as a function of ratio ranking in **Figure 2**. In the case of solution-processed graphene, there is significant variation with $\sigma_{dc,B}/\sigma_{op}$ ranging from 0.01 to ~15. The two highest ranked results were for networks of silver nanoparticle decorated graphene sheets, so these are not, strictly speaking, graphene films. Of these samples, the most promising film had $T \sim 80\%$ and $R_s \sim 250$ Ω/sq. We note that the highest graphene-only film displayed $\sigma_{dc,B}/\sigma_{op} \sim 1.3$. The relatively poor

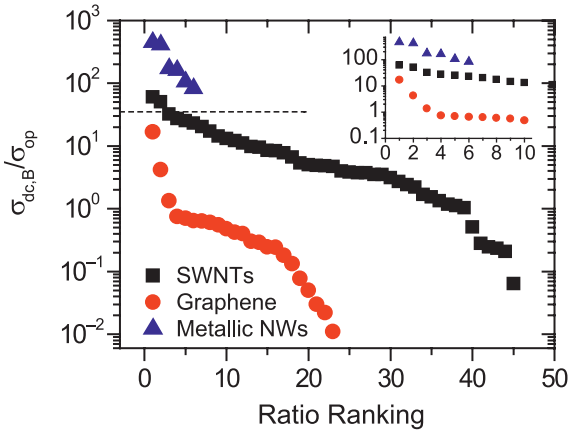

Figure 2. Bulk dc to optical conductivity ratio plotted in order of ratio ranking for solution-processed thin films prepared from metallic nanowires, single-walled carbon nanotubes, and graphene. The horizontal dashed line shows the value of $\sigma_{dc,B}/\sigma_{op} = 35$ required to reach the minimum industry standards of $T = 90\%$ and $R_s = 100\ \Omega$/sq. The inset shows the best performing samples for each material type.

performance of graphene networks is due to a combination[45] of low dc conductivity due to resistive inter-flake junctions[70] and the high optical conductivity of graphene.[71] In the case of nanotubes, the spread is significantly less, with $\sigma_{dc,B}/\sigma_{op}$ values ranging from ~0.1 to ~60. The best sample was for nanotubes deposited from superacids whose most promising film displayed $T \approx 91\%$ and $R_s \approx 60\ \Omega$/sq.[72] Looking at the 10 best values (Figure 2 inset), it is clear that the spread is very tight, with the top 10 varying in $\sigma_{dc,B}/\sigma_{op}$ from 12 to 60. This reflects the relative maturity of nanotube-based transparent conductor research and may suggest that this technology is approaching physical limits, possibly set by the high inter-nanotube junction resistance.[73] Turning to the data for metallic nanowire networks, while there are relatively few papers on these materials, the $\sigma_{dc,B}/\sigma_{op}$ values are very impressive, ranging from 106 to 453. We note that the sample with the highest $\sigma_{dc,B}/\sigma_{op}$ was a spray cast silver nanowire network, whose best film displayed $T \approx 85\%$ and $R_s \approx 33\ \Omega$/sq.[39] However, we note that a sample with lower $\sigma_{dc,B}/\sigma_{op}$ (but no percolative regime, see later in text) included one film with even more impressive properties: $T \approx 89\%$ and $R_s \approx 20\ \Omega$/sq.[38] The high values observed here are due to a combination of low inter-wire junction resistance[36,37] and low optical conductivity of these networks.[36]

This analysis clearly shows that only networks created from SWNTs produced using non-trivial processing (i.e., superacid-based processing) or metallic nanowires have surpassed the first requirement for a high-performance TC ($\sigma_{dc,B}/\sigma_{op} \geq 35$). As superacid dispersions will not readily lend themselves to industrial processing, we suggest that only metallic nanowire networks are suitable candidates for solution-processed high-performance TCs. It is worth noting that $\sigma_{dc,B}/\sigma_{op}$ is largely a material property; it is primarily controlled by the optical and electrical properties of the nanoconductors and the potential profile of the junction between them (and thus the junction resistance). This suggests that metallic nanowires qualify as candidates for high-performance TCs, while SWNTs and graphene networks currently do not, due to their intrinsic material properties. This is important, as such intrinsic properties will not be easy to modify. On the face of it, this suggests the metallic nanowire networks to be the obvious choice. However, we note that as the properties of high transparency films of metallic nanowires may be controlled by percolation, $\sigma_{dc,B}/\sigma_{op}$ may not accurately describe their properties. Thus, it is important to know whether technologically relevant films (i.e., $T > 90\%$) lie in the bulk or percolative regime.

To test this, we first needed to know where the crossover from bulk to percolative behavior occurred. From the published data we extracted the transmittance, T_x, and sheet resistance, R_x, at the crossover between the bulk and percolative regimes. These data are plotted in **Figure 3**. From this it is clear that for all materials, the crossover occurred at transmittances between 50% and 92%. In almost all cases, T_x was below 90%, meaning that any film displaying $T = 90\%$ almost always falls in the percolative regime. In addition, with the exception of the metallic nanowire data, almost all of the R_x data were >100 Ω/sq, showing that $T = 90\%$ and $R_s < 100\ \Omega$/sq cannot be achieved for the vast majority of samples.

In addition, we used the published data to estimate the resistance for a film with $T = 90\%$, $R_s^{T=90\%}$, for each data set (in some cases by extrapolation). We also noted whether the 90% film occurred in the bulk or percolative region of the (R_s, T)

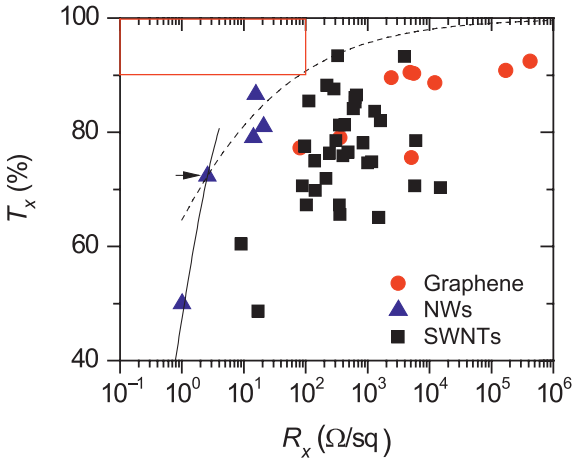

Figure 3. The crossover between bulk and percolative behavior. The boundary between the bulk and percolative regimes can be characterized by the transmittance, T_x, and sheet resistance, R_x, at the crossover. These are plotted in this figure for all three materials. The meaning of this crossover is illustrated for the point marked by the arrow. To the left of each data point, T is related to R_s for that material by the bulk expression (Equation 3), as shown by the solid line. However, to the right of each point, the $T(R_s)$ data are described by the percolative expression (Equation 5), as shown by the dashed line. The red box encloses the region required by industry for electrodes for high-performance displays or solar cells.

graph. These data are plotted in **Figure 4** as a function of the conductivity ratio ranking given in Figure 2. In each case, the data points where $T = 90\%$ film occurred in the bulk regime and are marked by a solid data point, while the percolation data are open circles. A number of things are of interest. First, for the various types of nanowire, the $T = 90\%$ film occurred in the percolative regime seven times out of eight. The one nanowire type that displayed no percolation regime also displayed the best individual film, reaching $T \approx 89\%$ and $R_s = 20\ \Omega$/sq, despite having a relatively low value of $\sigma_{dc,B}/\sigma_{op} = 173$.[38] For the SWNT data, the $T = 90\%$ film occurred in the percolative regime 66% of the time, while for graphene films, the rate was only 16%. This can be explained by noting that the percolative regime applies for films with a thickness $t < t_{min}$, where $t_{min} \approx 2.33D$. Here, D is the thickness of the smallest dimension of the nanomaterial (i.e., the diameter of the nanowire or nanotube bundle or the thickness of the graphene flake). As this dimension is generally large for nanowires ($D > 50$ nm), even relatively thick nanowire films can be percolative. However the thickness of a graphene flake is very small (~nm), which means only very thin films should be percolating. SWNTs fall between these two extremes. In addition, we note that when the $T = 90\%$ film is in the bulk regime, $R_s^{T=90\%}$ scales smoothly with the ranking, as expected from Equation 3. However, for films where the $T = 90\%$ film is in the percolating regime, $R_s^{T=90\%}$ shows much more scatter (because it also depends on t_{min} and n) and critically is always larger than would be expected for the equivalent bulk film. This illustrates the fact that percolation is very common and, when present, limits film performance.

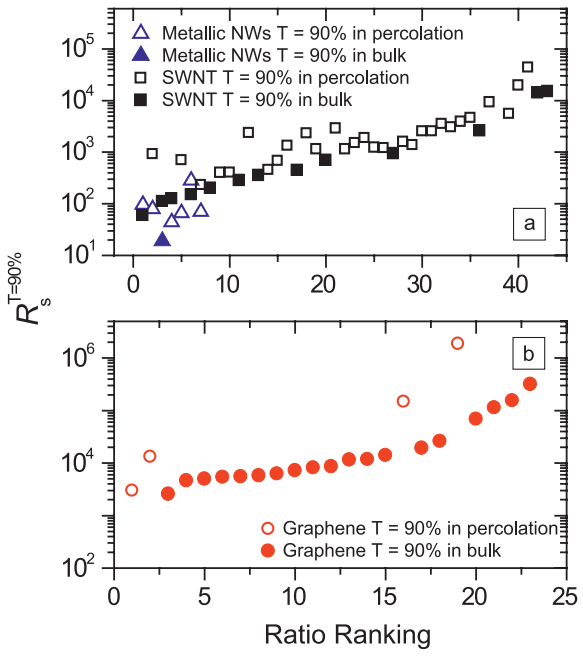

Figure 4. The sheet resistance expected for a film with $T = 90\%$, $R_s^{T=90\%}$, plotted as a function of the rankings for $\sigma_{dc,B}/\sigma_{op}$ (see Figure 2). In each plot, the solid data represent films where $T = 90\%$ would fall in the bulk regime, while the open symbols represent films where $T = 90\%$ would fall in the percolation regime. Note that the presence of percolation always increases $R_s^{T=90\%}$ above what would otherwise be expected. To avoid clutter, we have divided the data between nanowires and nanotubes (a) and graphene (b).

Given how often percolation is the limiting factor in nanostructured TCs, it is worth looking in more detail at Π and n, which were obtained by fitting published (R_s, T) data as described previously. In **Figure 5**, we plot Π as a function of n, for networks of graphene, SWNTs, and metallic nanowires. The data for SWNTs are widely spread, perhaps suggesting considerable variability between nanotube types and processing methods. In contrast, the metallic nanowire and graphene data follow elongated patterns sloping downward and upward, respectively. These patterns are consistent with Equations 5 and 6 and occur for values of $\sigma_{dc,B}/\sigma_{op}$ that are relatively high or low, respectively (typically the case for metallic nanowires or graphene networks). More importantly, by inserting $T = 90\%$ and $R_s = 100\ \Omega$/sq and rearranging Equation 5, we can plot a curve that separates films with $T > 90\%$ and $R_s < 100\ \Omega$/sq from those with $T < 90\%$ and $R_s > 100\ \Omega$/sq. This is shown as the dashed line (i.e., for a film to display $T > 90\%$ and $R_s < 100\ \Omega$/sq, its [n, Π] data must sit above this line). It is clear from these data that only the metallic nanowires surpass minimum industry standards for films where percolation controls the film properties. This is a very interesting result. It means that not only are metallic nanowires the only nanoconductors to fulfill the material requirements (i.e., $\sigma_{dc,B}/\sigma_{op} \geq 35$), but they are also the only nanoconductors to form sparse networks that are capable of achieving $T \geq 90\%$ and $R_s \leq 100\ \Omega$/sq. This is further evidence that metallic nanowires are the most promising nanoconductors for solution-processed TCs.

A number of papers have speculated on the dependence of the dc conductivity of networks of nanotubes on the nanotube

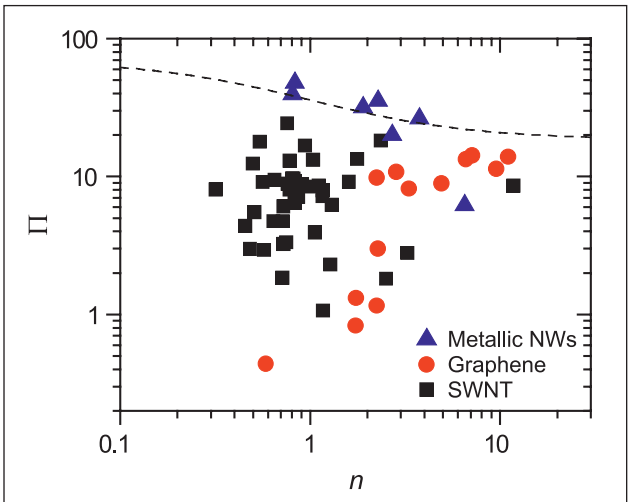

Figure 5. Percolation fit constants; the percolation figure of merit, Π, plotted as a function of the percolation exponent, n, for films of metallic nanowires, single-walled carbon nanotubes, and graphene. To achieve $T > 90\%$ and $R_s < 100\ \Omega$/sq, the data must fall above the dashed line on this graph (plotted using Equations 5 and 6).

bundle diameter. It is generally agreed that smaller diameter bundles result in more conducting paths, and therefore higher dc conductivity.[74,75] Two articles in particular have predicted power law diameter dependences: $\sigma_{dc,B} \propto D^{-n}$, where n has been suggested as either 2 (Reference 74) or 3 (Reference 75). These are important predictions, as they suggest that films with higher $\sigma_{dc,B}$, and hence higher $\sigma_{dc,B}/\sigma_{op}$, could be achieved by using smaller nanotube bundles (i.e., better exfoliated tubes). However, such power law dependence has not been conclusively demonstrated.[76] The published data collected during the preparation of this review allowed the examination of this question. As shown in Figure 3, data have been collected on the transmittance at the crossover from bulk to percolative behavior, T_x. This transmittance can be related to the thickness of the network at crossover, t_{min} via Equation 1, so long as the optical conductivity, σ_{op}, is known. While σ_{op} is not known particularly well for networks of metallic nanowires and is very scattered for graphene networks,[45] it has been measured by a number of groups to be between 15,000 and 22,000 S/m for nanotube networks.[35,64,77,78] Taking σ_{op} = 18,500 S/m, this allows us to use Equation 1 to estimate t_{min} for a range of SWNT networks, obtaining values between 11 and 130 nm. This is of interest, as t_{min} should approximately scale with nanotube diameter, D, as $t_{min} \approx 2.33D$. This allows us to use t_{min} as a proxy for bundle diameter. In this way, we can examine the diameter dependence of $\sigma_{dc,B}$ via that of $\sigma_{dc,B}/\sigma_{op}$, which we now know. Shown in **Figure 6**a is $\sigma_{dc,B}/\sigma_{op}$ plotted as a function of t_{min} for a range of SWNT networks (on the top axis is the estimated bundle diameter). Although the data are scattered (due to varying nanotube types, network morphologies), it is reasonably clear that smaller values of t_{min}, and so smaller bundle diameter, lead to larger $\sigma_{dc,B}/\sigma_{op}$. In addition, it can also be seen that the data are reasonably consistent with a power law of the form $\sigma_{dc,B} / \sigma_{op} \propto D^{-n}$ with $1 < n < 4$. These data are consistent with both power laws previously proposed.

However, it is important to remember that the technologically relevant parameter is not $\sigma_{dc,B}/\sigma_{op}$, but $R_s^{T=90\%}$. In most cases, $R_s^{T=90\%}$ is not controlled solely by $\sigma_{dc,B}/\sigma_{op}$ but also depends on t_{min}, σ_{op}, and n (Equations 5 and 6). Thus we test the dependence of $R_s^{T=90\%}$ on diameter in Figure 6b. From this graph, it is clear that smaller values of t_{min} (and so smaller D) lead to lower values of $R_s^{T=90\%}$ for SWNT networks, clearly illustrating the importance of good exfoliation. Previously, we have speculated that similar rules should apply to metallic nanowire networks. However, we note that the difference here is that we simply do not know enough about the optical conductivity of such networks. For example, if the optical conductivity increases with decreasing wire diameter, this effect may cancel out much of the advantage of using low diameter nanowires.

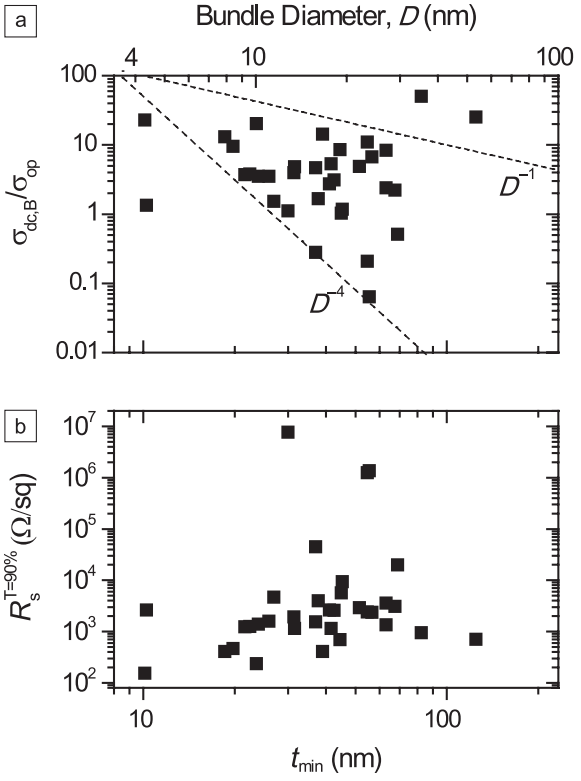

Figure 6. (a) The conductivity ratio, $\sigma_{dc,B}/\sigma_{op}$, and (b) the sheet resistance expected for a film with T = 90%, $R_s^{T=90\%}$, plotted as a function of t_{min}. Here, t_{min} is the film thickness where the transfer from bulk to percolation occurs. This was found by estimating the transmittance where the transition occurs, T_x, and using Equation 1 to convert to t_{min} (σ_{op} = 1.85 × 10^4 S/m in all cases). On the top axis is the estimated bundle diameter, D, calculated using $t_{min} \approx 2.33D$. In (a), the dashed lines illustrate D^{-4} and D^{-1} dependence. Note that only single-walled carbon nanotube films were considered.

Concluding remarks

We have reviewed current state-of-the-art transparent conducting (TC) thin films of nanoscale conductors prepared by solution processing. We have analyzed the published data for transmittance as a function of sheet resistance for networks of graphene, nanotubes, and metallic nanowires. In the majority of cases, there was a transition from bulk-like behavior to percolation behavior as the film thickness was reduced. In most cases, the technologically relevant films with $T \geq 90\%$ lie in the percolative regime. By fitting to known models, we extracted both bulk and percolative figures of merit for all samples. We found that only networks of metallic nanowires possess high enough figures of merit to qualify as high performance TCs (i.e., $T \geq 90\%$ and $R_s \leq 100$ Ω/sq). Finally, we have shown that at least for nanotube networks, the film performance scales with bundle diameter.

Networks of metallic nanowires are now very promising candidates for ITO replacement. A number of authors have reported metallic nanowire films with $T \geq 90\%$ and $R_s \leq 100$ Ω/sq.[37,38,41] In addition, these films can now be produced by industrially compatible methods, such as spray coating.[39] However, a number of hurdles remain. Adhesion of solution processed Ag nanowire films to substrates has been poor,[36] an issue that must be resolved before industrialization. In addition, scattering of

light due to the relatively large diameter of typical nanowires (50–100 nm) results in haze[42] which, while good for solar cells, will be detrimental to the performance of displays. In addition, commercially available Ag nanowires tend to be coated with an organic stabilizer. This is displaced locally from the junction region during network formation, giving excellent electrical contact at junctions while the remaining organic coating protects the nanowire surface from tarnishing (i.e., oxidizing). However, the temporal stability of these coatings is unknown, and if it degrades over time, the network conductivity is likely to suffer. Finally, although some work has begun,[40,41] it will be necessary to demonstrate temporally stable, high-performance networks of nanowires from cheap metals such as copper. Thus, if these hurdles can be addressed, the path forward is clear; formation of networks from low diameter nanowires may result in better optoelectrical properties[75] and should reduce haze. If the wires can be produced from copper with an appropriate, long-lasting, surface stabilizer, the next generation of high-performance TCs may be based on metallic nanowires.

Acknowledgments

We acknowledge the Science Foundation Ireland funded collaboration (SFI grant 03/CE3/M406s1) between Trinity College Dublin and Hewlett Packard, which has allowed this work to take place.

References

1. M. Batzill, U. Diebold, *Prog. Surf. Sci.* **79**, 47 (2005).
2. R.G. Gordon, *MRS Bull.* **25**, 52 (2000).
3. D.S. Hecht, L.B. Hu, G. Irvin, *Adv. Mater.* **23**, 1482 (2011).
4. D.R. Cairns, G.P. Crawford, *Proc. IEEE* **93**, 1451 (2005).
5. D.R. Cairns, R.P. Witte, D.K. Sparacin, S.M. Sachsman, D.C. Paine, G.P. Crawford, R.R. Newton, *Appl. Phys. Lett.* **76**, 1425 (2000).
6. Z. Chen, B. Cotterell, W. Wang, *Eng. Fract. Mech.* **69**, 597 (2002).
7. Y. Leterrier, L. Medico, F. Demarco, J.A.E. Manson, U. Betz, M.F. Escola, M.K. Olsson, F. Atamny, *Thin Solid Films* **460**, 156 (2004).
8. W. den Boer, G.S. Smith, *J. SID* **13**, 199 (2005).
9. M.W. Rowell, M.D. McGehee, *Energy Environ. Sci.* **4**, 131 (2011).
10. V. Scardaci, R. Coull, P. E. Lyons, D. Rickard, J.N. Coleman, *Small* **7** (18), 2621 (2011).
11. C. Schrage, S. Kaskel, *ACS Appl. Mater. Interfaces* **1**, 1640 (2009).
12. B. Dan, G.C. Irvin, M. Pasquali, *ACS Nano* **3**, 835 (2009).
13. S. De, P.E. Lyons, S. Sorrel, E.M. Doherty, P.J. King, W.J. Blau, P.N. Nirmalraj, J.J. Boland, V. Scardaci, J. Joimel, J.N. Coleman, *ACS Nano* **3**, 714 (2009).
14. H.Z. Geng, K.K. Kim, K.P. So, Y.S. Lee, Y. Chang, Y.H. Lee, *J. Am. Chem. Soc.* **129**, 7758 (2007).
15. L. Hu, D.S. Hecht, G. Gruner, *Nano Lett.* **4**, 2513 (2004).
16. Z.C. Wu, Z.H. Chen, X. Du, J.M. Logan, J. Sippel, M. Nikolou, K. Kamaras, J.R. Reynolds, D.B. Tanner, A.F. Hebard, A.G. Rinzler, *Science* **305**, 1273 (2004).
17. Z.R. Li, H.R. Kandel, E. Dervishi, V. Saini, Y. Xu, A.R. Biris, D. Lupu, G.J. Salamo, A.S. Biris, *Langmuir* **24**, 2655 (2008).
18. S. Manivannan, J.H. Ryu, J. Jang, K.C. Park, *J. Mater. Sci. - Mater. Electron.* **21**, 595 (2010).
19. S.F. Pei, J.H. Du, Y. Zeng, C. Liu, H.M. Cheng, *Nanotechnology* **20**, 235707 (2009).
20. G. Fanchini, S. Miller, L.B. Parekh, M. Chhowalla, *Nano Lett.* **8**, 2176 (2008).
21. B.B. Parekh, G. Fanchini, G. Eda, M. Chhowalla, *Appl. Phys. Lett.* **90**, 121913 (2007).
22. H.E. Unalan, G. Fanchini, A. Kanwal, A. Du Pasquier, M. Chhowalla, *Nano Lett.* **6**, 677 (2006).
23. B. Chandra, A. Afzali, N. Khare, M.M. El-Ashry, G.S. Tulevski, *Chem. Mater.* **22**, 5179 (2010).
24. Y. Wang, C.A. Di, Y.Q. Liu, H. Kajiura, S.H. Ye, L.C. Cao, D.C. Wei, H.L. Zhang, Y.M. Li, K. Noda, *Adv. Mater.* **20**, 4442 (2008).
25. Z.R. Li, H.R. Kandel, E. Dervishi, V. Saini, A.S. Biris, A.R. Biris, D. Lupu, *Appl. Phys. Lett.* **91**, 053115 (2007).
26. H. Tantang, J.Y. Ong, C.L. Loh, X.C. Dong, P. Chen, Y. Chen, X. Hu, L.P. Tan, L.J. Li, *Carbon* **47**, 1867 (2009).
27. H.Z. Geng, D.S. Lee, K.K. Kim, S.J. Kim, J.J. Bae, Y.H. Lee, *J. Korean Phys. Soc.* **53**, 979 (2008).
28. Y.T. Park, A.Y. Ham, J.C. Grunlan, *J. Mater. Chem.* **21**, 363 (2011).
29. H.Z. Geng, K.K. Kim, C. Song, N.T. Xuyen, S.M. Kim, K.A. Park, D.S. Lee, K.H. An, Y.S. Lee, Y. Chang, Y.J. Lee, J.Y. Choi, A. Benayad, Y.H. Lee, *J. Mater. Chem.* **18**, 1261 (2008).
30. S.B. Yang, B.S. Kong, J. Geng, H.T. Jung, *J. Phys. Chem. C* **113**, 13658 (2009).
31. D.W. Shin, J.H. Lee, Y.H. Kim, S.M. Yu, S.Y. Park, J.B. Yoo, *Nanotechnology* **20**, 475703 (2009).
32. A.A. Green, M.C. Hersam, *Nat. Nanotechnol.* **4**, 64 (2009).
33. A.A. Green, M.C. Hersam, *Nano Lett.* **8**, 1417 (2008).
34. A. Southard, V. Sangwan, J. Cheng, E.D. Williams, M.S. Fuhrer, *Org. Electron.* **10**, 1556 (2009).
35. E.M. Doherty, S. De, P.E. Lyons, A. Shmeliov, P.N. Nirmalraj, V. Scardaci, J. Joimel, W.J. Blau, J.J. Boland, J.N. Coleman, *Carbon* **47**, 2466 (2009).
36. S. De, T. Higgins, P.E. Lyons, E.M. Doherty, P.N. Nirmalraj, W.J. Blau, J.J. Boland, J.N. Coleman, *ACS Nano* **3**, 1767 (2009).
37. J.Y. Lee, S.T. Connor, Y. Cui, P. Peumans, *Nano Lett.* **8**, 689 (2008).
38. A.R. Madaria, A. Kumar, F.N. Ishikawa, C.W. Zhou, *Nano Res.* **3**, 564 (2010).
39. A.R. Madaria, A. Kumar, C.W. Zhou, *Nanotechnology* **22**, 245201 (2011).
40. A.R. Rathmell, S.M. Bergin, Y.L. Hua, Z.Y. Li, B.J. Wiley, *Adv. Mater.* **22**, 3558 (2010).
41. H. Wu, L.B. Hu, M.W. Rowell, D.S. Kong, J.J. Cha, J.R. McDonough, J. Zhu, Y.A. Yang, M.D. McGehee, Y. Cui, *Nano Lett.* **10**, 4242 (2010).
42. L.B. Hu, H.S. Kim, J.Y. Lee, P. Peumans, Y. Cui, *ACS Nano* **4**, 2955 (2010).
43. H.A. Becerril, J. Mao, Z. Liu, R.M. Stoltenberg, Z. Bao, Y. Chen, *ACS Nano* **2**, 463 (2008).
44. P. Blake, P.D. Brimicombe, R.R. Nair, T.J. Booth, D. Jiang, F. Schedin, L.A. Ponomarenko, S.V. Morozov, H.F. Gleeson, E.W. Hill, A.K. Geim, K.S. Novoselov, *Nano Lett.* **8**, 1704 (2008).
45. S. De, J.N. Coleman, *ACS Nano* **4**, 2713 (2010).
46. S. De, P.J. King, M. Lotya, A. O'Neill, E.M. Doherty, Y. Hernandez, G.S. Duesberg, J.N. Coleman, *Small* **6**, 458 (2010).
47. G. Eda, G. Fanchini, M. Chhowalla, *Nat. Nanotechnol.* **3**, 270 (2008).
48. T.K. Hong, D.W. Lee, H.J. Choi, H.S. Shin, B.S. Kim, *ACS Nano* **4**, 3861 (2010).
49. H. Yamaguchi, G. Eda, C. Mattevi, H. Kim, M. Chhowalla, *ACS Nano* **4**, 524 (2010).
50. C. Mattevi, G. Eda, S. Agnoli, S. Miller, K.A. Mkhoyan, O. Celik, D. Mostrogiovanni, G. Granozzi, E. Garfunkel, M. Chhowalla, *Adv. Funct. Mater.* **19**, 2577 (2009).
51. X. Wang, L.J. Zhi, N. Tsao, Z. Tomovic, J.L. Li, K. Mullen, *Angew. Chem. Int. Ed.* **47**, 2990 (2008).
52. G. Eda, Y.Y. Lin, S. Miller, C.W. Chen, W.F. Su, M. Chhowalla, *Appl. Phys. Lett.* **92**, 233305 (2008).
53. J.B. Wu, H.A. Becerril, Z.N. Bao, Z.F. Liu, Y.S. Chen, P. Peumans, *Appl. Phys. Lett.* **92**, 263302 (2008).
54. Y.W. Zhu, W.W. Cai, R.D. Piner, A. Velamakanni, R.S. Ruoff, *Appl. Phys. Lett.* **95**, 103104 (2009).
55. H.W. Tien, Y.L. Huang, S.Y. Yang, J.Y. Wang, C.C.M. Ma, *Carbon* **49**, 1550 (2011).
56. L.J. Cote, F. Kim, J.X. Huang, *J. Am. Chem. Soc.* **131**, 1043 (2009).
57. Y.K. Kim, D.H. Min, *Langmuir* **25**, 11302 (2009).
58. Y.Q. Liu, L. Gao, J. Sun, Y. Wang, J. Zhang, *Nanotechnology* **20**, 465605 (2009).
59. Y.Y. Liang, J. Frisch, L.J. Zhi, H. Norouzi-Arasi, X.L. Feng, J.P. Rabe, N. Koch, K. Mullen, *Nanotechnology* **20**, 434007 (2009).
60. X.L. Li, G.Y. Zhang, X.D. Bai, X.M. Sun, X.R. Wang, E. Wang, H.J. Dai, *Nat. Nanotechnol.* **3**, 538 (2008).
61. S. Biswas, L.T. Drzal, *Nano Lett.* **9**, 167 (2009).
62. X. Wang, L.J. Zhi, K. Mullen, *Nano Lett.* **8**, 323 (2008).
63. A.A. Green, M.C. Hersam, *Nano Lett.* **9**, 4031 (2009).
64. H.Z. Geng, D.S. Lee, K.K. Kim, G.H. Han, H.K. Park, Y.H. Lee, *Chem. Phys. Lett.* **455**, 275 (2008).
65. V. Scardaci, R. Coull, J.N. Coleman, *Appl. Phys. Lett.* **97** (2010).
66. N. Saran, K. Parikh, D.S. Suh, E. Munoz, H. Kolla, S.K. Manohar, *J. Am. Chem. Soc.* **126**, 4462 (2004).
67. M. Dressel, G. Gruner, *Electrodynamics of Solids: Optical Properties of Electrons in Matter* (Cambridge University Press, Cambridge, UK, 2002).
68. S. De, P.J. King, P.E. Lyons, U. Khan, J.N. Coleman, *ACS Nano* **4**, 7064 (2010).
69. D.S. Stauffer, A. Aharony, *Introduction to Percolation Theory* (Taylor & Francis, London, UK, 1994).

70. P.N. Nirmalraj, T. Lutz, S. Kumar, G.S. Duesberg, J.J. Boland, *Nano Lett.* **11**, 16 (2011).
71. R.R. Nair, P. Blake, A.N. Grigorenko, K.S. Novoselov, T.J. Booth, T. Stauber, N.M.R. Peres, A.K. Geim, *Science* **320**, 1308 (2008).
72. D.S. Hecht, A.M. Heintz, R. Lee, L.B. Hu, B. Moore, C. Cucksey, S. Risser, *Nanotechnology* **22**, 075201 (2011).
73. P.N. Nirmalraj, P.E. Lyons, S. De, J.N. Coleman, J.J. Boland, *Nano Lett.* **9**, 3890 (2009).
74. D. Hecht, L.B. Hu, G. Gruner, *Appl. Phys. Lett.* **89**, 133112 (2006).
75. P.E. Lyons, S. De, F. Blighe, V. Nicolosi, L.F.C. Pereira, M.S. Ferreira, J.N. Coleman, *J. Appl. Phys.* **104**, 044302 (2008).
76. D.H. Shin, H.C. Shim, J.W. Song, S. Kim, C.S. Hana, *Scr. Mater.* **60**, 607 (2009).
77. B. Ruzicka, L. Degiorgi, R. Gaal, L. Thien-Nga, R. Bacsa, J.P. Salvetat, L. Forro, *Phys. Rev. B* **61**, R2468 (2000).
78. A. Ugawa, J. Hwang, H.H. Gommans, H. Tashiro, A.G. Rinzler, D.B. Tanner, *Curr. Appl. Phys.* **1**, 45 (2001). □